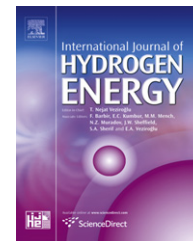


Available online at www.sciencedirect.com

SciVerse ScienceDirect

journal homepage: www.elsevier.com/locate/ijhe

Neural network hybrid model of a direct internal reforming solid oxide fuel cell

Kattiyapon Chaichana^a, Yaneeporn Patcharavorachot^b, Bhawasut Chutichai^a,
Dang Saebea^a, Suttichai Assabumrungrat^a, Amornchai Arpornwichanop^{a,c,*}

^a Department of Chemical Engineering, Faculty of Engineering, Chulalongkorn University, Bangkok 10330, Thailand

^b School of Chemical Engineering, Faculty of Engineering, King Mongkut's Institute of Technology Ladkrabang, Bangkok 10520, Thailand

^c Computational Process Engineering, Chulalongkorn University, Bangkok 10330, Thailand

ARTICLE INFO

Article history:

Received 13 August 2011

Received in revised form

7 October 2011

Accepted 11 October 2011

Available online 17 November 2011

Keywords:

Solid oxide fuel cell

Neural network

Hybrid model

Direct internal reforming

Performance analysis

ABSTRACT

A mathematical model is an important tool for analysis and design of fuel cell stacks and systems. In general, the complete description of fuel cells requires an electrochemical model to predict their electrical characteristics, i.e., cell voltage and current density. However, obtaining the electrochemical model is quite a difficult and complicated task as it involves various operational, structural and electrochemical reaction parameters. In this study, a neural network model was first proposed to predict the electrochemical characteristics of solid oxide fuel cell (SOFC). Various NN structures were trained based on the back-propagation feed-forward approach. The results showed that the NN with optimal structure reliably provides a good estimation of fuel cell electrical characteristics. Then, a neural network hybrid model of a direct internal reforming SOFC, combining mass conservation equations with the NN model, was developed to determine the distributions of gaseous components in fuel and air channels of SOFC as well as the performance of the SOFC in terms of power density and fuel cell efficiency. The effects of various key parameters, e.g., temperature, pressure, steam to carbon ratio, degree of pre-reforming, and inlet fuel flow rate on the SOFC performance under steady-state and isothermal conditions were also investigated. A combination of the first principle model and NN presents a significant advantage of predicting the SOFC performance with accuracy and less computational time.

Copyright © 2011, Hydrogen Energy Publications, LLC. Published by Elsevier Ltd. All rights reserved.

1. Introduction

A solid oxide fuel cell (SOFC) is considered a promising energy-conversion device for power generation. The flexibility to use various choices of fuel types (e.g., methane, methanol, ethanol, etc.) and the prospect for heat and power combined system are the main benefits of SOFC [1,2]. Moreover, a high

temperature operation of SOFC allows the endothermic steam reforming of fuel for hydrogen production to be carried out within the SOFC stack, which is referred to as an internal reforming SOFC (IR-SOFC). In IR-SOFC operation, the heat generated from an electrochemical reaction can internally supply to the endothermic steam reforming reaction, resulting in a higher energy efficiency of the SOFC system [3,4].

* Corresponding author. Department of Chemical Engineering, Faculty of Engineering, Chulalongkorn University, Bangkok 10330, Thailand. Tel.: +66 2 2186878; fax: +66 2 2186877.

E-mail address: amornchai.a@chula.ac.th (A. Arpornwichanop).

0360-3199/\$ – see front matter Copyright © 2011, Hydrogen Energy Publications, LLC. Published by Elsevier Ltd. All rights reserved.
doi:10.1016/j.ijhydene.2011.10.051

However, it is known that the operation of SOFC at high temperatures requires durable materials for cell components and thus, the high-cost SOFC fabrication is inevitable. Recently, a number of studies have been focused on intermediate-temperature SOFCs (IT-SOFCs) operating between 823 and 1073 K, which allows for a wider range of materials, more cost-effective fabrication, longer cell life, and shorter start-up period [4–8].

During the last several decades, many researchers have developed mathematical models of SOFCs in order to examine mass, heat and electrochemical processes occurred within the fuel cell stack, leading to a further improvement of fuel cell performance [4,8–12]. In general, SOFC models are governed by conservation equations and electrochemical model. The electrochemical model describing the mechanism of fuel conversion to electrical power plays an important role in analyzing the performance of SOFC by correlating current density with cell voltage and voltage losses found in fuel cells [13–16]. However, acquiring such a model is not an easy task as it involves complicated reaction and mass transport processes coupled with electrical characteristics of fuel cells. Furthermore, the electrochemical relation are dependent of the operation conditions, e.g., temperature, pressure, and fuel

and air compositions, and fuel cell physical properties, e.g., macro/micro-structures of electrodes and electrolyte, which include porosity, tortuosity, thickness of cell components and ionic and electronic conductivities. These parameters require specific knowledge and are difficult to be determined or can be even estimated but with less accuracy [16,17]. Due to the complexity of the electrochemical models of fuel cells, many previous studies have attempted to establish attractive alternative fuel cell models based on input–output relations to analyze fuel cell performance [18–25].

Neural network (NN) is regarded as one of the most effective techniques to be used for modeling complex processes. It can approximate a nonlinear relationship between input and output variables without the requirement of explicit mathematical representations. By using NN, it is unnecessary to have any prior knowledge about the relationships that exist among the states of the process [26]. Although a NN approach can be applied to explain the SOFC stack or the whole process of SOFCs [23–25], a hybrid model constructed from a basic first principle model coupled with a NN model should be considered since it can be used to describe some physical and chemical processes within the SOFC. It was reported that the combination of the first principle model with NN can provide

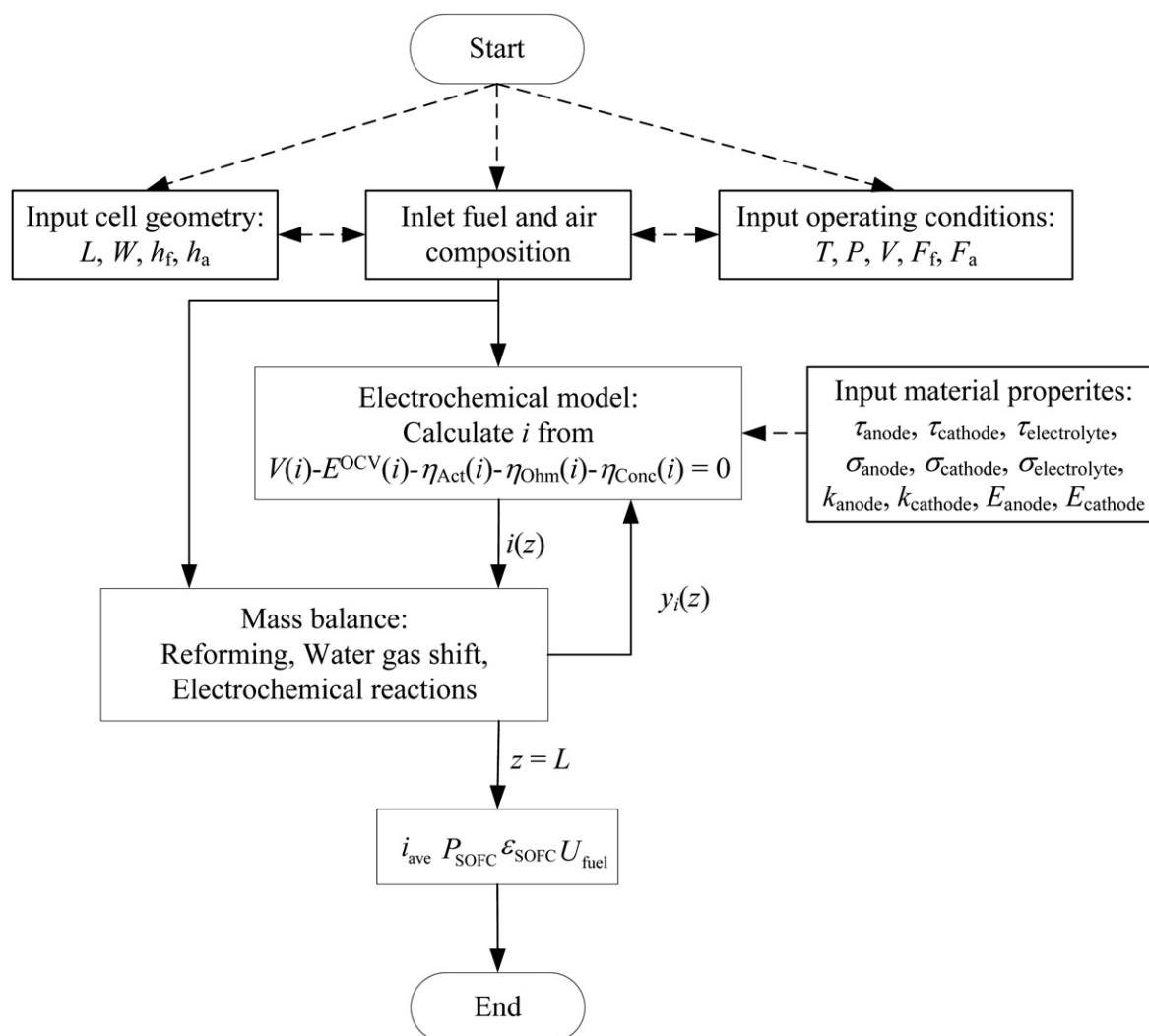


Fig. 1 – Computational algorithm for simulation of SOFC.

a good accuracy of process modeling with less computational time [27–30].

In this work, a NN hybrid model is developed to analyze a steady-state behavior of the SOFC operated under direct internal reforming. In such a modeling approach, NN is applied to learn the electrical characteristics of the SOFC. Due to the limited availability of experimental data over a wide range of operating conditions, the simulated data obtained from simulations of an electrochemical model are used for training the NN in this study. The training data has the following input parameters: operating temperature, mole fractions of H_2 and H_2O , and cell voltage, whereas the current density is considered as an output parameter. The reliability of the NN model is examined by comparing its prediction with the data obtained from the detailed electrochemical model. The developed NN model is incorporated with mass conservation models to describe the distribution of gaseous components in fuel and air channels of SOFC. The NN hybrid model is then employed to analysis the performance of SOFC with respect to various key operating parameters.

2. Neural network hybrid model of internal reforming SOFC

In general, the SOFC model at isothermal condition consists of mass conservation equations that describe changes in gaseous compositions along the fuel cell channels and an electrochemical model that relates the fuel and air compositions to fuel cell voltage, current density, and all electrochemical-related variables. Fig. 1 presents a flow diagram of numerical algorithm for steady-state simulation of SOFC. The model input parameters are cell geometries, operating conditions, and inlet fuel and air compositions, whereas the material property data are further required for the electrochemical model. The mass balance equations are used to determine the axial distribution of gas compositions along the fuel and air channels. Due to the variation in gas compositions, the current density generated inside the SOFC, which is computed from the electrochemical model, is also varied with the flow direction. When the distribution of current density is known, the average current density generated can be computed and therefore, the performance of SOFC in terms of power density, fuel cell efficiency, and fuel utilization, can be determined as the cell voltage is given. As seen in Fig. 1, there are large numbers of important parameters for solving the current density. These include cell component thickness and material properties (i.e., electrode/electrolyte conductivities, electrode exchange-current densities) which are difficult to be accurately determined.

In this work, the NN hybrid model of SOFC is proposed and its structure is shown in Fig. 2. The NN hybrid model of SOFC combines the first principle model with the NN. The SOFC system model is described by a set of mass balance equations and the electrochemical model is represented by the NN. The NN model is used to learn the relationship between certain input and output data. The input data are operating temperature (T), mole fractions of H_2 and H_2O (y_{H_2} , y_{H_2O}), and cell voltage (V), whereas the current density (i) is the output data. When the NN is implemented via a hybrid modeling approach, it can estimate the current density that is employed to compute the variation of gas composition along the cell length of SOFC through solving mass balance equations. As seen in Fig. 2, the input model parameters used in this work are cell dimension and operating conditions.

2.1. Mass balance equations of SOFC

Considering the SOFC operated with direct internal reforming of methane, there are five chemical reactions taking place within an SOFC stack:

Fuel channel:



Air channel:



Overall electrochemical reaction:



A mathematical model of an anode-supported planar SOFC with direct internal reforming operation (DIR) presented in this study was developed based on the following assumptions: (1) steady-state operation, (2) one-dimensional variation of parameters in x -direction, (3) uniform temperature and total pressure over the model geometry, and (4) constant cell voltage along the cell coordinate. By performing mass balances, the differential equations describing the change of component concentrations in fuel and air channels along the axial direction can be written as follows:

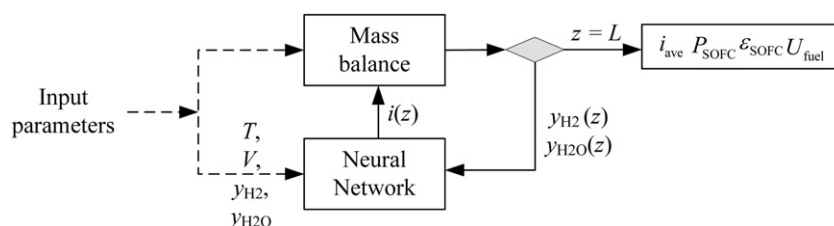


Fig. 2 – Structure of a neural network hybrid model.

Fuel channel ($i = \text{CH}_4, \text{H}_2\text{O}, \text{CO}, \text{H}_2,$ and CO_2):

$$\frac{dC_{i,f}}{dx} = \frac{1}{u_f} \sum_{j \in \{(1),(2),(5)\}} \nu_{i,j} R_j \frac{1}{h_f} \quad (6)$$

Air channel ($i = \text{O}_2,$ and N_2):

$$\frac{dC_{i,a}}{dx} = \frac{1}{u_a} \nu_{i,(5)} R_{(5)} \frac{1}{h_a} \quad (7)$$

where C_i is the molar concentration of component i (mol m^{-3}), $\nu_{i,j}$ is the stoichiometric coefficient of component i in reaction j and R_j is the rate of reaction j ($\text{mol m}^{-2} \text{s}^{-1}$). u_f and u_a are the fuel and air velocities (m s^{-1}), respectively. h_f and h_a are the height of fuel and air channels (m), respectively.

The rate expressions for the methane steam reforming, water gas shift and the electrochemical reactions are shown as follows [31,32]:

$$R_{(1)} = k_0 p_{\text{CH}_4} \exp\left(-\frac{E_a}{RT}\right) \quad (8)$$

$$R_{(2)} = k_{\text{WGSR}} \left(p_{\text{CO}} p_{\text{H}_2\text{O}} - \frac{p_{\text{CO}_2} p_{\text{H}_2}}{K_{\text{eq}}} \right) \quad (9)$$

$$R_{(3)} = R_{(4)} = R_{(5)} = \frac{i}{2F} \quad (10)$$

where k_0 is the pre-exponential constant ($=4274 \text{ mol s}^{-1} \text{ m}^{-2} \text{ bar}^{-1}$) and E_a is the activation energy ($=82 \text{ kJ mol}^{-1}$) for steam reforming reaction, respectively [31], k_{WGSR} is the pre-exponential factor ($\text{mol m}^{-3} \text{ Pa}^{-2} \text{ s}^{-1}$) and K_{eq} is the equilibrium constant for water gas shift reaction as follows:

$$k_{\text{WGSR}} = 0.0171 \exp\left(-\frac{103,191}{RT}\right) \quad (11)$$

$$K_{\text{eq}} = \exp(-0.2935Z^3 + 0.6351Z^2 + 4.1788Z + 0.3169), Z = \frac{1000}{T(K)} - 1 \quad (12)$$

2.2. Electrochemical model

An electrochemical model is used to predict the local cell voltage, current density, and fuel cell performance-related variables, i.e., power density, fuel and air utilizations, and fuel cell efficiency. The theoretical voltage, referred to the open-circuit voltage (E^{OCV}), is the maximum voltage that can be achieved from the SOFC under constant operating conditions. It can be determined by the Nernst equation. However, in real operation, the operating cell voltage at a closed-circuit condition is always lower than E^{OCV} due to the occurrence of various voltage losses. There are three main voltage losses taking place in the fuel cell: (1) activation loss (η_{Act}) which is a voltage loss associated with the electrochemical reactions at the electrode surfaces, (2) ohmic loss (η_{Ohm}) which is a voltage loss caused by the resistance to the flow of ions in electrolyte and to the flow of electrons through electrically conductive fuel cell components, and (3) concentration loss which is voltage losses due to the transport of gaseous through the porous electrodes.

Considering the detailed electrochemical model, these various voltage losses are strongly influenced by different parameters which include the operating conditions (i.e., temperature, pressure and fuel and air composition) and the physical properties of the fuel cell (i.e., porosity, tortuosity, electronic conductivity and thickness of the electrodes, ionic conductivity and thickness of the electrolyte). Accordingly, the equations for describing activation, ohmic and concentration losses have been differently proposed [13–17]. The electrochemical model of SOFC used in this study is summarized in Table 1.

2.3. Neural network for prediction of electrochemical characteristics

In this work, a multilayer feed-forward NN which represents a special form of a connectionist model that performs mapping from an input space to an output space is applied to predict the current density generated by an SOFC. For optimal design of the NN, the data for training the NN are divided into three different sets: training, validation and testing data sets. It is emphasized here that in general, the experimental data of SOFC are used for NN training; however, with their limited availability for various operating conditions, the simulated data obtained from numerical simulations using a detailed electrochemical model as mentioned in Section 2.2 (Eqs. (13)–(21)) are assumed to be used instead. Although various

Table 1 – Electrochemical model of SOFC.

$$\text{Open-circuit voltage } (E^{\text{OCV}}): \\ E^{\text{OCV}} = E^0 + \frac{RT}{2F} \ln\left(\frac{p_{\text{H}_2} p_{\text{O}_2}^{0.5}}{p_{\text{H}_2\text{O}}}\right) \quad (13)$$

$$\text{Operating voltage } (V): \\ V = E^{\text{OCV}} - (\eta_{\text{ohm}} + \eta_{\text{act}} + \eta_{\text{conc}}) \quad (14)$$

$$\text{Activation overpotential } (\eta_{\text{act}}): \\ i = i_{0,\text{electrode}} \left[\exp\left(\frac{\alpha n F}{RT} \eta_{\text{act,electrode}}\right) - \exp\left(-\frac{(1-\alpha) n F}{RT} \eta_{\text{act,electrode}}\right) \right] \quad (15)$$

$$i_{0,\text{electrode}} = \frac{\mathfrak{R}T}{nF} k_{\text{electrode}} \exp\left(-\frac{E_{\text{electrode}}}{RT}\right) \quad (16)$$

$$\text{Ohmic loss } (\eta_{\text{ohm}}): \\ \eta_{\text{Ohm}} = i \sum \left(\frac{\tau_i}{\sigma_i}\right) = i \left(\frac{\tau_{\text{anode}}}{\sigma_{\text{anode}}} + \frac{\tau_{\text{electrolyte}}}{\sigma_{\text{electrolyte}}} + \frac{\tau_{\text{cathode}}}{\sigma_{\text{cathode}}}\right) \quad (17)$$

$$\text{Concentration overpotential } (\eta_{\text{conc}}): \\ \eta_{\text{Conc}} = \frac{RT}{2F} \ln\left(\frac{p_{\text{H}_2\text{O,TPB}} p_{\text{H}_2}}{p_{\text{H}_2\text{O}} p_{\text{H}_2,\text{TPB}}}\right) + \frac{RT}{4F} \ln\left(\frac{p_{\text{O}_2}}{p_{\text{O}_2,\text{TPB}}}\right) \quad (18)$$

$$\text{where} \\ p_{\text{H}_2,\text{TPB}} = p_{\text{H}_2,f} - \frac{RT \tau_{\text{anode}}}{2FD_{\text{eff,anode}}} i \quad (19)$$

$$p_{\text{H}_2\text{O,TPB}} = p_{\text{H}_2\text{O},f} + \frac{RT \tau_{\text{anode}}}{2FD_{\text{eff,anode}}} i \quad (20)$$

$$p_{\text{O}_2,\text{TPB}} = P - (P - p_{\text{O}_2,a}) \exp\left(\frac{RT \tau_{\text{cathode}}}{4FD_{\text{eff,cathode}}} i\right) \quad (21)$$

Table 2 – Parameters used in the electrochemical model of SOFC [10].

τ_{anode}	500 μm	k_{anode}	$6.54 \times 10^{11} \Omega^{-1} \text{m}^{-2}$
τ_{cathode}	50 μm	k_{cathode}	$2.35 \times 10^{11} \Omega^{-1} \text{m}^{-2}$
$\tau_{\text{electrolyte}}$	20 μm	E_{anode}	140 kJ mol^{-1}
σ_{anode}	$80 \times 10^3 \Omega^{-1} \text{m}^{-1}$	E_{cathode}	137 kJ mol^{-1}
σ_{cathode}	$8.4 \times 10^3 \Omega^{-1} \text{m}^{-1}$	$D_{\text{eff,anode}}$	$3.66 \times 10^{-5} \text{m}^2 \text{s}^{-1}$
$\sigma_{\text{electrolyte}}$	$33.4 \times 10^3 \exp(-10\ 300/T) \Omega^{-1} \text{m}^{-1}$	$D_{\text{eff,cathode}}$	$1.37 \times 10^{-5} \text{m}^2 \text{s}^{-1}$

SOFC models have been proposed to predict the electrical characteristics of SOFC, they require many kinetic parameters. Even these parameters can be determined or estimated from experimental data, they are likely to have substantial errors. In the future, the experimental SOFC data covered a wide range of operating conditions are expected to be used for NN training.

Table 2 shows the values of parameters used in the SOFC electrochemical model. To generate the data sets, the main operational variables of a fuel cell, i.e., operating temperatures, mole fractions of H_2 and H_2O , and operating cell voltage are varied in the range of 873–1273 K, 0.1–0.9, and 0–1.1 V, respectively, and the values of the corresponding current density are recorded as the output. It is assumed that the mole fraction of O_2 at the air channel is kept constant as a high air-to-fuel ratio is employed under the nominal operation of fuel cells. All the data obtained are then normalized by Z-score standardization for achieving a good performance of the NN model. Levenberg–Marquardt back-propagation algorithm with the early stopping mechanism is used to train the multilayer feed-forward NN [33,34]. To optimize the network structure, the number of hidden layers and neurons are altered during the training process. A mean square error (MSE) is used as a criterion for the NN selection and also for the stopping of weights and biases adjustment. The training process is finished when the network provided a satisfied error ($\text{MSE} \leq 1 \times 10^{-4}$).

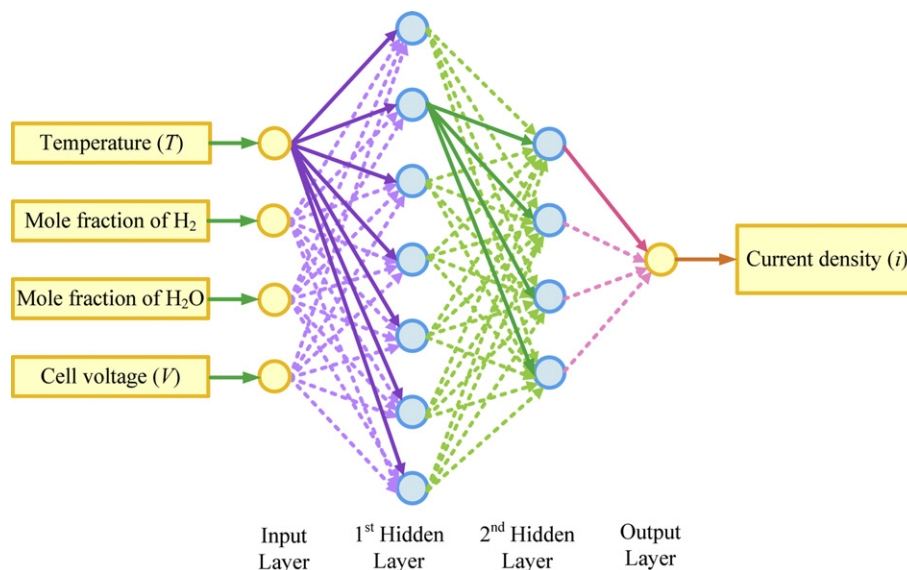
3. Results and discussions

This section is divided in two subsections: Section 3.1 presents the optimal structure of the NN model obtained from methodology proposed in Section 2.3. The performance analysis of an anode-supported planar SOFC-DIR is performed by using the NN hybrid model of SOFC and explained in Section 3.2.

3.1. Neural network structure

An optimal structure of NN model that gives the minimum value of the MSE is considered to be an appropriate NN model. From simulation results, it is found that the optimum architecture of the NN model for prediction of the fuel cell current density consists of four layers; one input, two hidden and one output layers, as shown in Fig. 3. As seen in Fig. 3, the input layer consists of four nodes which are the operating temperature, the mole fractions of H_2 and H_2O , and cell voltage, respectively. The two hidden layers are composed of seven and four nodes with the log-sigmoid transfer function, whereas the output layer consists of one output node with a linear transfer function to predict the current density produced by SOFC.

To evaluate the performance characteristics of SOFC obtained from NN model, the predictions of current density based on the use of the NN model at different cell voltages and temperatures are compared with the actual values obtained from the detailed electrochemical model of SOFC. It can be seen from Fig. 4 that the NN model provides an accurate prediction of the current density (R^2 99.985%). It is noted that the cell performance decreases drastically with decreasing the operating temperature. This is mainly caused by an increase in both the ohmic and the activation losses. The effect of the concentration loss is highly pronounced at a high operating temperature. Moreover, this simulation results are consistent with other literatures [14,15,35].

**Fig. 3 – Optimal structure of a neural network model.**

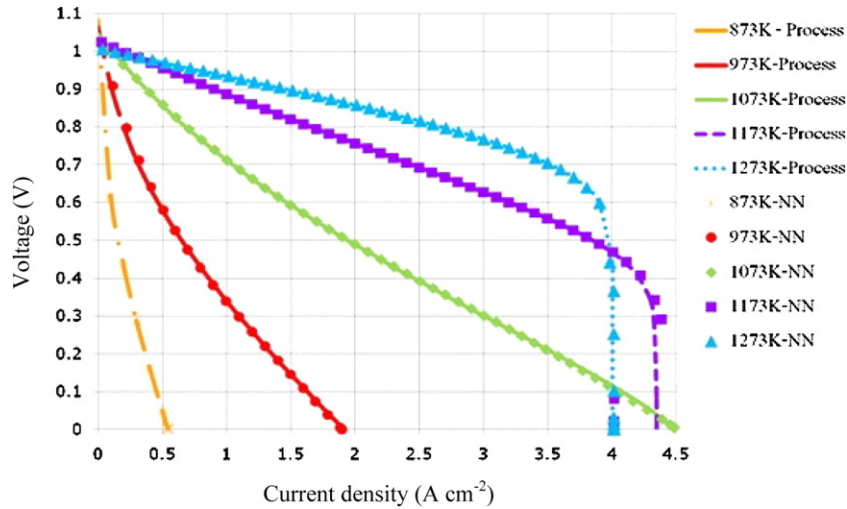


Fig. 4 – Comparison of SOFC electrical characteristics obtained from NN model and electrochemical model.

3.2. Steady-state SOFC performance

In this section, the performance of an anode-supported SOFC fed by methane under direct internal reforming and isothermal conditions is investigated based on the developed NN hybrid model. Table 3 summarizes the values of model input: cell dimensions and operating conditions used in this work. The inlet fuel composition given in Table 3 is based on the synthesis gas derived from a gas mixture of steam and methane at a ratio of 2 after 10% pre-reforming whereas air consisting of 21% O₂, 79% N₂ is used as an oxidant. When the NN model is applied to replace the electrochemical model and integrated with mass balance equations, the model equations of SOFC consist of a set of ordinary differential (Eqs. (6) and (7)) and algebraic equations (Eqs. (8)–(12)). The mass balances can determine the gas composition distribution of each component in the gas channels. Due to the variation in gas compositions along the fuel and air channels, the local current density changes with the distance and can be estimated by

the NN model. The average current density (i_{ave}) obtained is calculated by integration of the current density distribution along the whole length of the cell channel. The steady-state performance in terms of power density (P_{SOFC}), fuel cell efficiency (ϵ_{SOFC}) and fuel utilization (U_{fuel}) can be determined as follows:

$$P_{SOFC} = i_{ave} V \quad (22)$$

$$\epsilon_{SOFC} = \frac{i_{ave} VLW}{(y_{CH_4}^{in} LHV_{CH_4} + y_{H_2}^{in} LHV_{H_2} + y_{CO}^{in} LHV_{CO}) F_f} \times 100\% \quad (23)$$

$$U_{fuel} = \frac{i_{ave} LW}{2F(4y_{CH_4}^{in} + y_{H_2}^{in} + y_{CO}^{in}) F_{H_2}} \quad (24)$$

where L and W are the length and width of cell, $y_{CH_4}^{in}$, $y_{H_2}^{in}$ and y_{CO}^{in} are the mole fractions of methane, hydrogen and carbon monoxide at the inlet of fuel cell, LHV_{CH_4} , LHV_{H_2} and LHV_{CO} are the lower heating values of methane, hydrogen and carbon monoxide, respectively.

Table 3 – Model parameters used in the performance analysis of an anode-supported SOFC-DIR.

Parameters	Value
Operating conditions	
Operating temperature, T	750 °C
Operating pressure, P	1.0 atm
Inlet molar flow rate of fuel, F_f	0.0015 s ⁻¹
Inlet molar flow rate of air, F_a	0.015 s ⁻¹
Air composition	21% O ₂ , 79% N ₂
Fuel composition	28.1% CH ₄ , 56.7% H ₂ O,
(steam/carbon 2, 10% pre-reforming)	0.5% CO, 12% H ₂ , and 2.7% CO ₂
Dimensions of cell element	
Cell length, L	0.4 m
Cell width, W	0.1 m
Fuel channel height, h_f	1 mm
Air channel height, h_a	1 mm

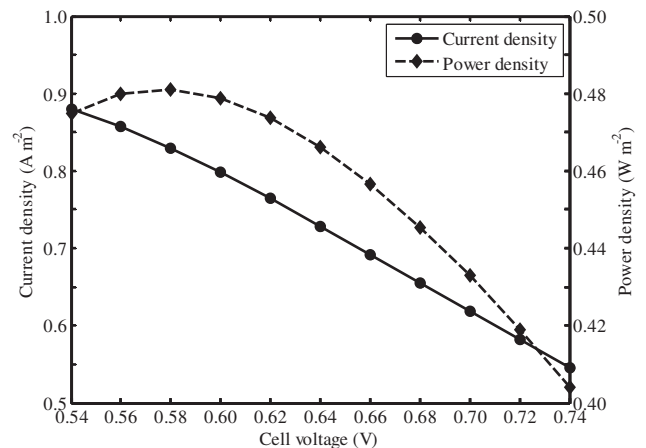


Fig. 5 – Performance characteristics of an anode-supported SOFC at different cell voltages.

Table 4 – Electrical characteristics of SOFC under the standard condition.

Cell voltage (V)	Average current density (A cm^{-2})	Power density (W cm^{-2})	Fuel cell efficiency (%)	Fuel utilization (%)
0.54	0.8793	0.4748	49.52	97.23
0.56	0.8569	0.4799	50.04	94.75
0.58	0.8296	0.4811	50.17	91.72
0.60	0.7982	0.4789	49.94	88.25
0.62	0.7641	0.4738	49.40	84.49
0.64	0.7284	0.4662	48.61	80.54
0.66	0.6919	0.4566	47.62	76.50
0.68	0.6551	0.4454	46.45	72.43
0.70	0.6184	0.4329	45.14	68.37
0.72	0.5821	0.4191	43.70	64.36
0.74	0.5462	0.4042	42.15	60.40

Before simulations of an anode-supported planar SOFC-DR are performed, its current-voltage characteristics are investigated to find a suitable operation condition. The current density and power density as a function of cell voltage in range of 0.54–0.74 V is presented in Fig. 5. Table 4 shows the values of average current density, power density, fuel cell

efficiency and fuel utilization. From the simulation results, it is found that an anode-supported SOFC can produce the maximum power density of 0.48 W cm^{-2} when the operating cell voltage is 0.58 V. However, at this condition, the fuel utilization is quite high (90%). In this study, the fuel cell operated at the cell voltage of 0.64 V is considered a suitable value as it shows a good compromise on power density and fuel utilization.

Under a standard condition, when the cell voltage of 0.64 V is specified, the distributions of gas composition in the fuel and air channels and the current density can be determined as presented in Fig. 6. Since high inlet CH_4 content and fast reaction rate of steam reforming result in the consumption of CH_4 and H_2O and the production of H_2 and CO at the entrance of the SOFC, as shown in Fig. 6a. When CH_4 is completely consumed, the electrochemical reactions become important and thus, H_2 and O_2 are more consumed while H_2O is more produced. At the exit of the fuel cell channel, the fuel stream consists of 0.10% CH_4 , 68.9% H_2O , 3.9% CO , 11.1% H_2 and 16.0% CO_2 , whereas the oxidant stream consists of 16.8% O_2 and 83.2% N_2 . Fig. 6b demonstrates the current density distribution along the fuel cell length. It can be seen that the current density sharply increases at the inlet and continuously

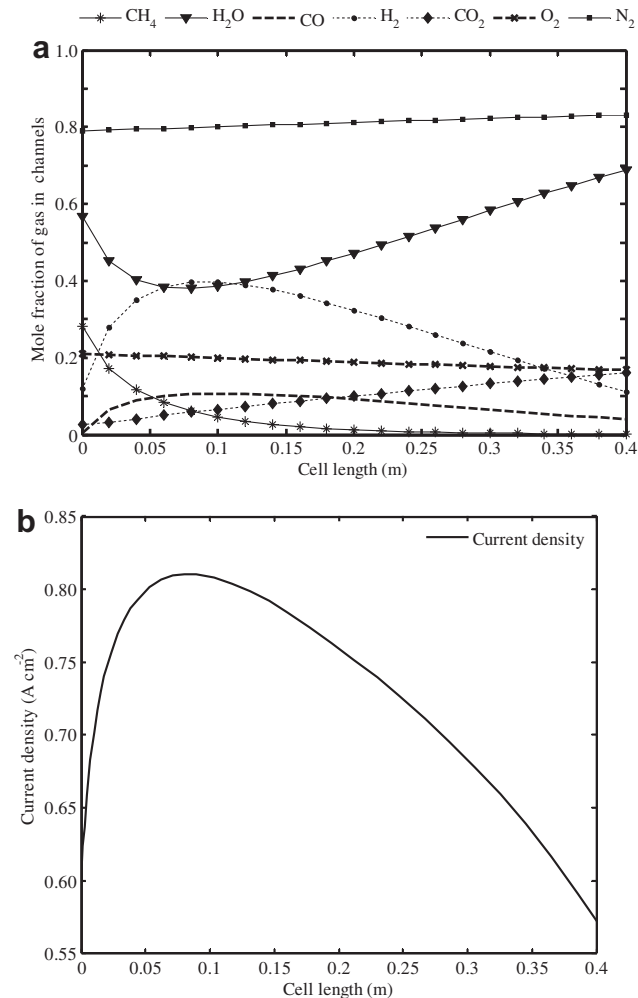


Fig. 6 – Distributions of mole fraction of gaseous components in fuel cell channels (a) and current density (b) along the fuel cell length.

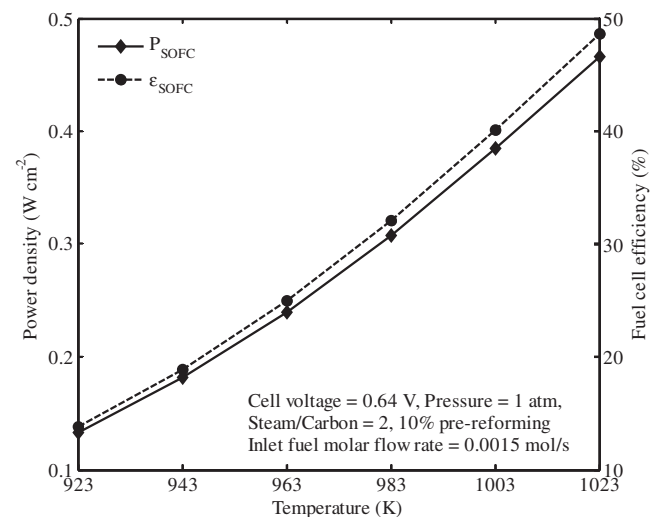


Fig. 7 – Effect of operating temperature on power density and fuel cell efficiency.

decreases toward the fuel cell outlet. The average current density is 0.728 A cm^{-2} . As a result, a power density of 0.466 W cm^{-2} , fuel cell efficiency of 58.61% and fuel utilization of 80.54% are achieved.

Furthermore, the effects of operating conditions such as temperature, pressure, steam to carbon molar ratio, degree of pre-reforming and inlet fuel molar flow rate, on SOFC performance are analysed under steady-state and isothermal operations. Fig. 7 presents the power density and fuel cell efficiency of the anode-supported SOFC as a function of operating temperatures varied from 923 to 1023 K. As expected, the SOFC performance can be improved when the operating temperature increases. An increase in the fuel cell temperatures causes high electrochemical reaction and the consumption of fuel. Since current density is more generated, the power density and fuel cell efficiency are enhanced. In addition, the operating temperature has strongly impact on the individual voltage losses as reported in the literatures [14,15]. It was also found that increasing the operating temperature causes a decrease in voltage losses, particularly the ohmic and activation losses.

Fig. 8 shows the power density and fuel cell efficiency as a function of operating pressures. The simulation results obtained from the NN hybrid model demonstrate that an increase in pressure from 0.5 to 3 atm can improve both the power density and fuel cell efficiency. At higher operating pressure, the partial pressure of H_2 in the fuel channel and O_2 in the air channel increases and therefore higher current density can be achieved. Besides the influence of partial pressure of reactant, the SOFC performance generally increases due to the fact that H_2 and O_2 can easily diffuse into the reaction site at the electrode–electrolyte interface under high pressure operation, which in turn decreases the concentration loss [15].

Fuel composition is one of the key parameters that has influence on the SOFC performance and needs to be considered. The effect of the steam/carbon molar ratio on the power density and fuel cell efficiency of the anode-supported SOFC is shown in Fig. 9. The steam/carbon ratio of feed stream to

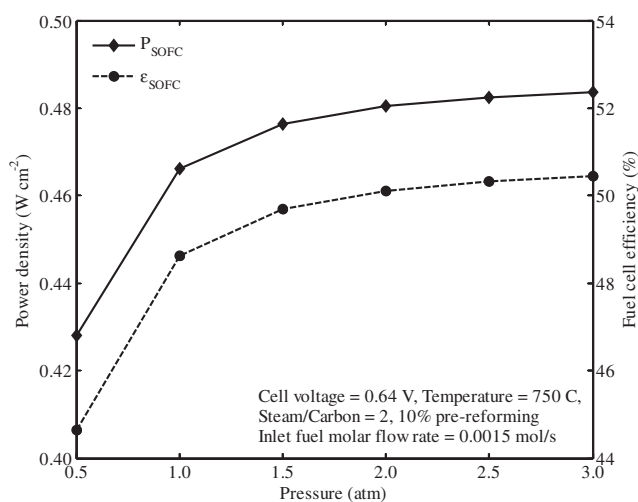


Fig. 8 – Effect of operating pressure on power density and fuel cell efficiency.

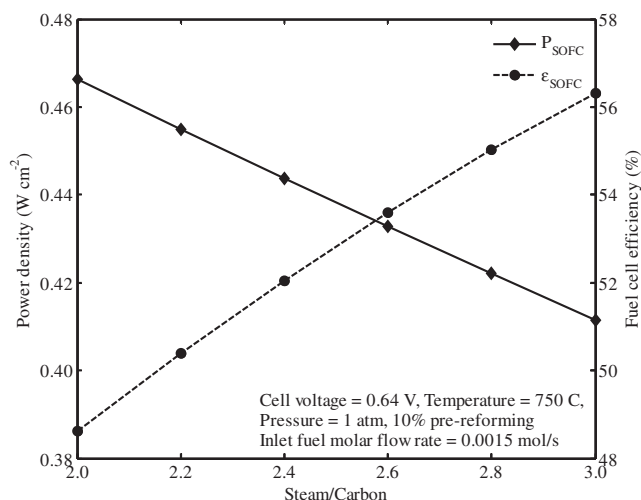


Fig. 9 – Effect of steam/carbon ratio on power density and fuel cell efficiency.

a pre-reformer is varied from 2 to 3. It means that the fuel stream to the SOFC has less fraction of H_2 but higher fraction of H_2O . This leads to the decreased rate of the electrochemical reaction, resulting in the reduction of current density and thus, the power density is also reduced. However, the fuel cell efficiency shows an opposite trend. This is because the increased steam/carbon ratio decreases the total fuel molar flow rate at the SOFC inlet used to produce current. Nevertheless, the reduction of the inlet fuel flow rate is lower, compared with the generation of current density and thus, the fuel cell efficiency is enhanced.

The effect of the degree of pre-reforming of CH_4 on power density and fuel cell efficiency is investigated, as demonstrated in Fig. 10. The degree of pre-reforming of methane at 10, 20, 30, 40 and 50% is studied. It should be noted that a higher degree of pre-reforming results in an increase in the H_2 composition in the fuel stream. In general, higher content of hydrogen in the SOFC fuel increases the open-circuit

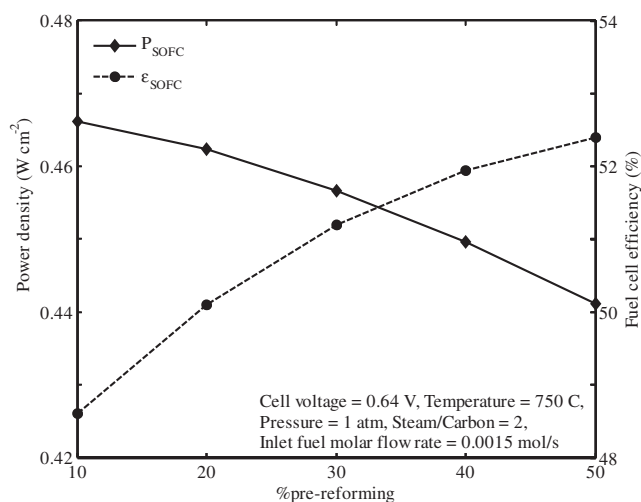


Fig. 10 – Effect of degree of pre-reforming on power density and fuel cell efficiency.

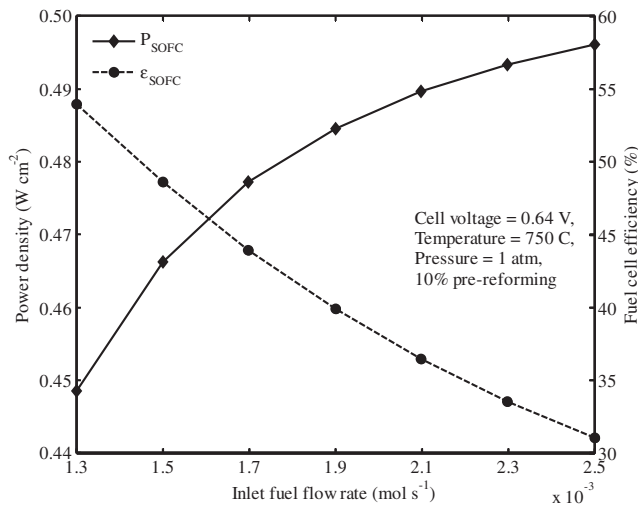


Fig. 11 – Effect of inlet fuel flow rate on power density and fuel cell efficiency.

voltage and current density and thus, higher power density is expected. However, the simulation results, as shown in Fig. 10, present an opposite trend. This can be explained that as H₂ is more consumed, the concentration loss becomes a dominant loss and the current density that can be locally drawn drops considerably to maintain a constant voltage. As a consequence, the power density decreases with increasing the methane pre-reforming level. However, the fuel cell efficiency is enhanced because of a decrease in inlet fuel molar flow rate according to more fuel utilization.

The effect of inlet molar flow rate of fuel on the power density and the fuel cell efficiency is investigated in range of 0.0013–0.0025 mol s⁻¹ (Fig. 11). From the simulation results, it can be seen that although higher molar flow rate of fuel leads to an increase in current density (referred to the power density), it has a reverse effect on fuel cell efficiency. In our previous work [4], it was reported that the conversion of chemical energy in fuel to electrical energy reduces when the molar flow rate of fuel increase. This causes the fuel having less residence time within the fuel cell for a complete electrochemical reaction and thus, the fuel cell efficiency is considerably decreased.

4. Conclusions

A neural network hybrid model of SOFC that combines a first principle model with a NN model was proposed in this work. The SOFC system is described by a set of mass balance equations to determine the distribution of gas composition in fuel cell whereas the electrochemical model is represented by the NN to estimate a current density. The simulated data obtained from simulations of the detailed electrochemical model was employed to train the NN model based on a back-propagation approach. It was found that the optimal structure of the NN for predicting the current density consists of one input layer with following four nodes: temperature, mole

fractions of H₂ and H₂O, and cell voltage; two hidden layers with seven and four nodes; and one output layer with one node of current density, respectively. The optimal NN structure reliably provides a good estimation of fuel cell electrical characteristics. Then, the developed NN hybrid model of SOFC was employed to evaluate the steady-state performance of an anode-supported planar SOFC. Under a standard condition, it was found that the average current density of 0.728 A cm⁻², power density of 0.466 W cm⁻², fuel cell efficiency of 58.61% and fuel utilization of 80.54% can be obtained at the cell voltage of 0.64 V. The performance analysis of SOFC with respect to effects of temperature, pressure, steam/carbon ratio, degree of pre-reforming of methane, and inlet fuel flow rate were performed. It was found that the increases of operating temperature, pressure, steam/carbon ratio, and degree of pre-reforming can improve the electrical efficiency of SOFC whereas the effect of inlet fuel molar flow rate presents an opposite trend.

Acknowledgements

K. Chaichana would like to thank the Office of the Higher Education Commission, Thailand for their grant support under the program “Strategic Scholarships for Frontier Research Network for the Ph.D. Program Thai Doctoral degree” for this research.

Support from the Thailand Research Fund, the Higher Education Research Promotion and National Research University Project of Thailand, Office of the Higher Education Commission (EN280A) and the Special Task Force for Activating Research (STAR), Chulalongkorn University Centenary Academic Development Project is gratefully acknowledged.

Nomenclature

$D_{\text{eff,anode}}$	Electrode effective gas diffusivity coefficient in the anode, m ² s ⁻¹
$D_{\text{eff,cathode}}$	Electrode effective gas diffusivity coefficient in the cathode, m ² s ⁻¹
$E_{\text{electrode}}$	Activation energy of the exchange-current density, kJ mol ⁻¹
E^{OCV}	Open-circuit voltage (OCV), V
$E_{\text{H}_2}^0$	Open-circuit potential at the standard pressure and temperature for the hydrogen oxidation reaction, V
F	Faraday’s constant, C mol ⁻¹
F_a	Molar flow rate of the air, mol s ⁻¹
F_f	Molar flow rate of the fuel, mol s ⁻¹
h_a	Air channel height, m
h_f	Fuel channel height, m
$i_{\text{ave},i}$	Average and local current density, A m ⁻²
$i_{0,\text{electrode}}$	Exchange-current density, A m ⁻²
K_{eq}	Equilibrium constant for water gas shift reaction
k_0	Pre-exponential constant for reforming reaction, mol s ⁻¹ m ⁻² bar ⁻¹
k_{WGSR}	Pre-exponential factor for water gas shift reaction, mol s ⁻¹ m ⁻³ Pa ⁻²

L	Cell length, m
LHV	Lower heating value, kJ mol ⁻¹
n	Number of electrons participating in the electrochemical reaction
P	Pressure, atm
p _i	Partial pressure of component i, atm
p _{i,TPB}	Partial pressure of gas component i at the three-phase boundaries, kPa
R	Gas constant, kJ mol ⁻¹ K ⁻¹
T	Temperature, K
V	Operating cell voltage, V

Greek symbols

α	Transfer coefficient
η _{act}	Activation loss, V
η _{con}	Concentration loss, V
η _{ohm}	Ohmic loss, V
σ _{anode}	Conductivity of anode, Ω ⁻¹ m ⁻¹
σ _{cathode}	Conductivity of cathode, Ω ⁻¹ m ⁻¹
σ _{electrolyte}	Conductivity of electrolyte, Ω ⁻¹ m ⁻¹
τ _{anode}	Anode thickness, m
τ _{cathode}	Cathode thickness, m
τ _{electrolyte}	Electrolyte thickness, m

Subscripts

a	Air channel
act	Activation
conc	Concentration
f	Fuel channel
i	Component
ohm	Ohmic

REFERENCES

- [1] Xue X, Tang J, Sammes N, Du Y. Dynamic modeling of single tubular SOFC combining heat/mass transfer and electrochemical reaction effects. *Journal of Power Sources* 2005;142:211–22.
- [2] Patcharavorachot Y, Paengjuntuek W, Assabumrungrat S, Arpornwichanop A. Performance evaluation of combined solid oxide fuel cells with different electrolytes. *International Journal of Hydrogen Energy* 2010;35:4301–10.
- [3] Peters R, Dahl R, Kluttgen U, Palm C, Stolten D. Internal reforming of methane in solid oxide fuel cell systems. *Journal of Power Sources* 2002;106:238–44.
- [4] Arpornwichanop A, Chalermpanchai N, Patcharavorachot Y, Assabumrungrat S, Tade M. Performance of an anode-supported solid oxide fuel cell with direct-internal reforming of ethanol. *International Journal of Hydrogen Energy* 2009;34:7780–8.
- [5] Leng YJ, Chan SH, Khor KA, Jiang SP. Performance evaluation for anode-supported solid oxide fuel cells with thin film YSZ electrolyte. *International Journal of Hydrogen Energy* 2004;29:1025–33.
- [6] Xin X, Lu Z, Huang X, Sha X, Zhang Y, Su W. Anode-supported solid oxide fuel cell based on dense electrolyte membrane fabricated by filter-coating. *Journal of Power Sources* 2006;159:1158–61.
- [7] Musa A, Paepe MD. Performance of combined internally reformed intermediate/high temperature SOFC cycle compared to internally reformed two-staged intermediate-temperature SOFC cycle. *International Journal of Hydrogen Energy* 2008;33:4665–72.
- [8] Aguiar P, Chadwick D, Kershenbaum L. Modelling of an indirect internal reforming solid oxide fuel cell. *Chemical Engineering Science* 2002;57:1665–77.
- [9] Yakabe H, Hishinuma M, Uratani M, Matsuzaki Y, Yasuda I. Evaluation and modeling of performance of anode-supported solid oxide fuel cell. *Journal of Power Sources* 2000;86:423–31.
- [10] Aguiar P, Adjiman CS, Brandon NP. Anode-supported intermediate-temperature direct internal reforming solid oxide fuel cell. I: Model-based steady-state performance. *Journal of Power Sources* 2004;138:120–36.
- [11] Hernandez-Pacheco E, Mann MD, Hutton PN, Singh D, Martin KE. A cell-level model for a solid oxide fuel cell operated with syngas from a gasification process. *International Journal of Hydrogen Energy* 2005;30:1221–33.
- [12] Kakaç S, Pramuanjaroenkij A, Zhou XY. A review of numerical modeling of solid oxide fuel cells. *International Journal of Hydrogen Energy* 2007;32:761–86.
- [13] Chan SH, Khor KA, Xia ZT. A complete polarization model of a solid oxide fuel cell and its sensitivity to the change of cell component thickness. *Journal of Power Sources* 2001;93:130–40.
- [14] Ni M, Leung MKH, Leung DYC. Parametric study of solid oxide fuel cell performance. *Energy Conversion and Management* 2007;48:1525–35.
- [15] Patcharavorachot Y, Arpornwichanop A, Chuachuensuk A. Electrochemical study of a planar solid oxide fuel cell: Role of support structures. *Journal of Power Sources* 2008;177:254–61.
- [16] Zhu H, Kee RJ. A general mathematical model for analyzing the performance of fuel-cell membrane-electrode assemblies. *Journal of Power Sources* 2003;117:61–74.
- [17] Suwanwarangkul R, Croiset E, Fowler MW, Douglas PL, Entchev E, Douglas MA. Performance comparison of Fick's, dusty-gas and Stefan–Maxwell models to predict the concentration overpotential of a SOFC anode. *Journal of Power Sources* 2003;122:9–18.
- [18] Zervas PL, Tatsis A, Sarimveis H, Markatos NCG. Development of a novel computational tool for optimizing the operation of fuel cells systems: application for phosphoric acid fuel cells. *Journal of Power Sources* 2008;185:345–55.
- [19] Lee WY, Park GG, Yang TH, Yoon YG, Kim CS. Empirical modeling of polymer electrolyte membrane fuel cell performance using artificial neural networks. *International Journal of Hydrogen Energy* 2004;29:961–6.
- [20] Ou S, Achenie Luke EK. A hybrid neural network model for PEM fuel cells. *Journal of Power Sources* 2005;140:319–30.
- [21] Arriagada J, Olausson P, Selimovic A. Artificial neural network simulator for SOFC performance prediction. *Journal of Power Sources* 2002;112:54–60.
- [22] Chávez-Ramírez AU, Muñoz-Guerrero R, Durón-Torres SM, Ferraro M, Brunaccini G, Sergi F. High power fuel cell simulator based on artificial neural network. *International Journal of Hydrogen Energy* 2010;35:12,125–12,133.
- [23] Wu XJ, Zhu XJ, Chao GY, Tu HY. Modeling a SOFC stack based on GA-RBF neural network identification. *Journal of Power Sources* 2007;167:145–50.
- [24] Saengrung A, Abtahi A, Zilouchian A. Neural network model for a commercial PEM fuel cell system. *Journal of Power Sources* 2007;172:749–59.
- [25] Milewski J, Swirski K. Modelling the SOFC behaviours by artificial neural network. *International Journal of Hydrogen Energy* 2009;34:5546–53.
- [26] Psychogios DC, Ungar LH. Direct and indirect model-based control using artificial neural networks. *Industrial & Engineering Chemistry Research* 1991;30:2564–73.

- [27] Qi H, Zhou X-G, Liu L-H, Yuan W-K. A hybrid neural network-first principles model for fixed-bed reactor. *Chemical Engineering Science* 1999;54:2521–6.
- [28] Ng CW, Hussain MA. Hybrid neural network—prior knowledge model in temperature control of a semi-batch polymerization process. *Chemical Engineering and Processing* 2004;43:559–70.
- [29] Chen L, Hontoir Y, Huang D, Zhang J, Morrisc AJ. Combining first principles with black-box techniques for reaction systems. *Control Engineering Practice* 2004;12: 819–26.
- [30] Zahedi G, Elkamel A, Lohi A, Jahanmirid A, Rahimpor MR. Hybrid artificial neural network—first principle model formulation for the unsteady-state simulation and analysis of a packed bed reactor for CO₂ hydrogenation to methanol. *Chemical Engineering Journal* 2005;115:113–20.
- [31] Achenbach E, Riensche E. Methane/steam reforming kinetics for solid oxide fuel cells. *Journal of Power Sources* 1994;52: 283–8.
- [32] Haberman BA, Young JB. Three-dimensional simulation of chemically reacting gas flows in the porous support structure of an integrated-planar solid oxide fuel cell. *International Journal of Heat and Mass Transfer* 2004;47:3617–29.
- [33] Daosud W, Thitayasook P, Arpornwichanop A, Kittisupakorn P, Hussain MA. Neural network inverse model based controller for the control of a steel picking process. *Computers and Chemical Engineering* 2005;29:2110–9.
- [34] Demuth H, Beale M. *Neural Network Toolbox Userguide*, Version 4; 2004.
- [35] Zhao F, Virkar AV. Dependence of polarization in anode-supported solid oxide fuel cells on various cell parameters. *Journal of Power Sources* 2005;141:79–95.